AFRL-OSR-VA-TR-2014-0268

PREDICTIONS FROM C/NOFS PLANAR LANGMUIR

Emanoel Costa
FACULDADES CATOLICAS

09/05/2014
Final Report

Air Force Research Laboratory
AF Office Of Scientific Research (AFOSR)/ IOS
Arlington, Virginia 22203
Air Force Materiel Command

REPORT DOCUMENTATION PAGE

Form Approved
OMB No. 0704-0188

1. REPORT DATE *(DD-MM-YYYY)*	**2. REPORT TYPE**	**3. DATES COVERED** *(From - To)*
25-08-2014	FINAL PERFORMANCE REPORT	from 01-12-2011 to 31-05-2014

4. TITLE AND SUBTITLE

Equatorial scintillation predictions from C/NOFS Planar Langmuir Probe electron density fluctuation data

5a. CONTRACT NUMBER

5b. GRANT NUMBER
FA9550-12-1-0031

5c. PROGRAM ELEMENT NUMBER

6. AUTHOR(S)

Emanoel Costa

5d. PROJECT NUMBER

5e. TASK NUMBER

5f. WORK UNIT NUMBER

7. PERFORMING ORGANIZATION NAME(S) AND ADDRESS(ES)

FACULDADES CATÓLICAS - Pontifícia Universidade Católica do Rio de Janeiro (PUC-Rio)
Rua Marquês de São Vicente 225
22451-900 Rio de Janeiro RJ Brazil

8. PERFORMING ORGANIZATION REPORT NUMBER

9. SPONSORING / MONITORING AGENCY NAME(S) AND ADDRESS(ES)

Air Force Office of Scientific Research
875 N Randolph St. Room 3112
Arlington VA 22203 USA

10. SPONSOR/MONITOR'S ACRONYM(S)

11. SPONSOR/MONITOR'S REPORT NUMBER(S)

12. DISTRIBUTION / AVAILABILITY STATEMENT

Approved for Public Release

13. SUPPLEMENTARY NOTES

The main objective of the work was the application of a propagation model based on in-situ measurements ion density irregulariti

14. ABSTRACT

The main objective of the work was the application of a propagation model based on in-situ measurements ion density irregularities to estimate the scintillation index S4. Initially, the results from a statistical analysis show how the values of the standard deviation DNi of the ion density fluctuations measured by the Planar Langmuir Probe (PLP) onboard the C/NOFS satellite were distributed, as functions of several combinations of several geophysical parameters. Considering the instant and position of detection of a sample of DNi as well as Vdrift, the model determined the instant of time when the sample reached the surface defined by the slant ray path and the intercepted magnetic field lines. Next, DNi was scaled for altitude using the observed average ion density profile. The scaled value of DNi, fixed power spectral density parameters and layer thickness were used to generate a horizontal random phase screen. Finally, a numerical algorithm was used to propagate a wave front to the ground and to estimate S4. The results from the calculations were compared with corresponding scintillation measurements by a 244-MHz Scintillation Network Decision Aid (SCINDA) receiver at Ancon, Peru for validation of a purely space-based scintillation detection, mapping and prediction model.

15. SUBJECT TERMS

16. SECURITY CLASSIFICATION OF:			**17. LIMITATION OF ABSTRACT**	**18. NUMBER OF PAGES**	**19a. NAME OF RESPONSIBLE PERSON**
a. REPORT	**b. ABSTRACT**	**c. THIS PAGE**		11	Emanoel Costa
					19b. TELEPHONE NUMBER *(include area code)*
					+ 55 21 35271682

PONTIFÍCIA UNIVERSIDADE CATÓLICA
DO RIO DE JANEIRO

FINAL PERFORMANCE REPORT

Equatorial scintillation predictions from C/NOFS Planar Langmuir Probe electron density fluctuation data

Principal Investigator: Emanoel Paiva de Oliveira Costa
+55 21 35271682
epoc@cetuc.puc-rio.br

Affiliation: Centro de Estudos em Telecomunicações (CETUC)
Pontifícia Universidade Católica do Rio de Janeiro (PUC-Rio)
Rua Marquês de São Vicente 225
22451-900 Rio de Janeiro RJ Brazil

Agreement Number: FA95550-12-1-0031

Program Manager: Dr. James Fillerup
AFOSR/IO
(703) 588-1777
james.fillerup@afosr.af.mil

Covered Dates: 01 December 2011 to 31 May 2014

Emanoel Costa
Centro de Estudos em Telecomunicações/CETUC
Rua Marquês de São Vicente, 225 – Gávea
22451-900 Rio de Janeiro - RJ – Brasil
Tel: 55 21 3527 1682; Fax: 55 21 3527 1154
E-mail: epoc@cetuc.puc-rio.br

PONTIFÍCIA UNIVERSIDADE CATÓLICA
DO RIO DE JANEIRO

FINAL PERFORMANCE REPORT

Equatorial scintillation predictions from C/NOFS Planar Langmuir Probe electron density fluctuation data

Emanoel Paiva de Oliveira Costa

Centro de Estudos em Telecomunicações (CETUC)
Pontifícia Universidade Católica do Rio de Janeiro (PUC-Rio)
Rua Marquês de São Vicente 225
22451-900 Rio de Janeiro RJ Brazil

Objectives: The main objectives of the proposed work were the identification of high-elevation orbits of the Communication/Navigation Outage Forecasting System (C/NOFS) satellite over a selected receiving station, followed by the application of a scintillation model to detected near-overhead irregularities to estimate the scintillation index S_4. The results from the calculations were compared with corresponding scintillation measurements by a 244-MHz Scintillation Network Decision Aid (SCINDA) receiver for validation of a purely space-based scintillation detection, mapping and prediction model.

Status of effort: The objectives of the work were reached. The radio wave scattering model was developed; a source code was implemented in the Fortran 77 language and tested. It was also applied to a phase screen characterized from one-second values of the standard deviation of ion density fluctuations measured by the Planar Langmuir Probe (PLP) onboard the C/NOFS satellite during its high-elevation orbits over Ancon, Peru (11.8° S, 77.2° W) to predict the scintillation index S_4 (the standard deviation of $I/\langle I \rangle$, where I is the received intensity and $\langle I \rangle$ its average value) at the VHF SCINDA frequency (244 MHz). Model predictions were compared with S_4 measurements by the same receiver.

Accomplishments/New Findings: Initially, a statistical analysis of the standard deviation of the ion density measured by the Planar Langmuir Probe (PLP) onboard the C/NOFS satellite was performed, to guide the selection of parameter values for the scintillation calculations. The PLP data are immediately available in individual daily files with 1-Hz resolution, but high-resolution data (512 Hz) are also available on request. Each 1-s record, corresponding to approximately 7.5 km, associates the Universal Time (s) to the corresponding average ion density N_i (cm^{-3}), standard deviation of the ion density ΔN_i (cm^{-3}), ratio $\Delta N_i/N_i$, as well as satellite latitude (degrees), longitude (degrees), and altitude (km). These records are obtained from the corresponding high-resolution data. PLP data from two different years (01 October 2008 to 30 September 2009 and 01 January 2012 to 31 December 2012) were selected for analysis. The first

Emanoel Costa
Centro de Estudos em Telecomunicações/CETUC
Rua Marquês de São Vicente, 225 – Gávea
22451-900 Rio de Janeiro - RJ – Brasil
Tel: 55 21 3527 1682; Fax: 55 21 3527 1154
E-mail: epoc@cetuc.puc-rio.br

data set corresponds to solar minimum conditions and the second one is as close to solar maximum conditions of solar cycle 24 as possible at the time of the analysis.

The results from the analysis, described and discussed in publication (2) listed below, show how the values of the standard deviation of the ion density ΔN_i (cm^{-3}) that exceeded levels $\log(\Delta N_i) > 3.5$ and $\log(\Delta N_i) > 4.5$ are statistically distributed, as functions of several combinations of the following parameters: (i) solar activity; (ii) altitude range; (iii) longitude sector; (iv) local time interval; (v) geomagnetic latitude interval; and (vi) season. The effects from the solar activity are represented by the differences between the results from the two selected years. Four local-time intervals {[18 LT, 21 LT); [21 LT, 24 LT); [00 LT, 03 LT); [03 LT, 06 LT)} and four seasons (days 34 to 125 for the March equinox, 126 to 216 for the June solstice, 217 to 307 for the September equinox and 308 to 33 for the December solstice) are considered. To study the altitude distribution of the values of ΔN_i that exceed the specified thresholds, four equal-size ranges are assumed: [400 km, 500 km); [500 km, 600 km); [600 km, 700 km); and [700 km, 800 km). Samples of ΔN_i corresponding to satellite positions outside these intervals are discarded. This selection of altitude intervals, in addition to keeping uniformity, also takes into account the fact that, with age, the C/NOFS satellite no longer reaches the initial apogee (850 km). Nine uneven longitude sectors are selected: South American West [270°-300°), South American East [300°-325°), Atlantic [325°-343°), African West [343°-030°), African East [030°-060°), Indian [060°-090°), Asian [090°-130°), Pacific West [130°-170°), and Pacific East [170°-270°). The magnetic latitude ψ is approximately determined from the relationship $\tan \psi = (1/2) \tan I_m$, where the magnetic inclination I_m is obtained from version 11 of the International Geomagnetic Reference Field model (IGRF-11) (International Association of Geomagnetism and Aeronomy, Working Group V-MOD, 2010) for the corresponding C/NOFS satellite position. To study the magnetic latitude distribution of the values of ΔN_i that exceed the specified thresholds, three equal-size intervals are considered: [-20°, -10°], [-5°, 5°], and [+10°, +20°]. Irregularities outside these intervals are not considered by magnetic latitude studies.

Publication (2) established that the dependences of the probability distributions of the absolute value of the standard deviation ΔN_i on the above parameters, directly relevant to scintillation-oriented studies, cannot be accurately inferred from those of the ratio $\Delta N_i/N_i$, analyzed by researchers associated with previous scientific satellite missions. Additionally, statistical studies of ΔN_i using in situ data from a wide altitude range in the equatorial topside ionospheric F region have not been previously reported. The results described in Figure 1, which exhibits the probability distributions of ΔN_i as functions of altitude ranges and longitude sectors, are particularly relevant to the present report. Panel 1(a) shows that the irregularities with $\log(\Delta N_i) > 3.5$ are rare above 500 km during the year 2008-2009, with the exception of those in the South American West and East sectors. Even for these two sectors, the probabilities decrease very fast (by factors approximately greater than five) between the two lowest altitude ranges.

For the year 2012, the irregularities with $\log(\Delta N_i) > 3.5$ reach the highest altitude range [700 km, 800 km) with relatively small but non negligible probabilities for all the sectors. Table 1 shows the results from a least-square fit of the exponential trendline $Pr_a(h) = Pr_a \exp(-ah)$ to the

Emanoel Costa
Centro de Estudos em Telecomunicações/CETUC
Rua Marquês de São Vicente, 225 – Gávea
22451-900 Rio de Janeiro - RJ – Brasil
Tel: 55 21 3527 1682; Fax: 55 21 3527 1154
E-mail: epoc@cetuc.puc-rio.br

data from each longitudinal sector of panel 1(b), where h (km) is the average height of each altitude range (450 km, 550 km, 650 km, and 750 km, respectively). The first three columns of Table 1 show the longitudinal sectors and the associated values of the parameters Pr_a and a, respectively. The fourth column displays the values of the coefficient of determination R^2, which is a number from 0 to 1 that reveals how closely the values estimated by the trendline are to the measured data. A trendline is most reliable when its R^2 value is at or near 1. The fifth column shows the probabilities $Pr_a(450\ km)$ calculated by the trendline at 450 km. The last column lists the values estimated from the data for the lowest altitude range [400 km, 500 km), also displayed in the corresponding bin of Figure 1(b). The high R^2 values and a comparison between corresponding numbers in the last two columns of Table 1 indicate that, for each longitude sector, an exponential trendline provides a reasonable description of the decrease with height of the probability of irregularities with $\log(\Delta N_i) > 3.5$ observed during the year 2012.

Table 1. Results from the Least Square Fit of the Exponential Trendline $Pr_a(h) = Pr_a\, exp(-ah)$ to Data of Figure 1(b). A Trendline is Most Reliable when its R^2 Value ($0 \leq R^2 \leq 1$) in the Fourth Column is at or Near 1. The Column Pr_{data} Lists the Values of the Bin [400 km, 500 km) of Figure 1(b).

Longitude Sector	$\boldsymbol{Pr_a}$	$\boldsymbol{a}$	$\boldsymbol{R^2}$	$Pr_a(450\ km)$	$\boldsymbol{Pr_{data}}$
SAmerica West	1.3358	0.0104	0.9755	0.0124	0.0102
SAmerica East	0.6566	0.0085	0.9798	0.0143	0.0122
Atlantic	0.3646	0.0080	0.9875	0.0100	0.0089
Africa West	0.4299	0.0084	0.9973	0.0098	0.0093
Africa East	1.2070	0.0108	0.9969	0.0094	0.0088
India	1.0674	0.0109	0.9934	0.0079	0.0072
Asia	2.1116	0.0119	0.9841	0.0100	0.0082
Pacific West	4.4543	0.0133	0.9921	0.0112	0.0098
Pacific East	5.6211	0.0135	0.9761	0.0129	0.0103

Panel 1(c) shows that the irregularities with $\log(\Delta N_i) > 4.5$ detected during the year 2012 peak in the lowest altitude range [400 km, 500 km) for all longitude sectors. Most are very rare above 600 km. The same holds for the strong irregularities observed above 500 km from the African East to the Pacific West sectors. The exceptions are the ones associated with South American East sector. Indeed, the probabilities related to this sector are clearly the greatest ones for each altitude range, up to 700 km.

In summary, the above results do not support the assumption of a thick irregularity layer for propagation studies associated with the years 2008-2012.

Emanoel Costa
Centro de Estudos em Telecomunicações/CETUC
Rua Marquês de São Vicente, 225 – Gávea
22451-900 Rio de Janeiro - RJ – Brasil
Tel: 55 21 3527 1682; Fax: 55 21 3527 1154
E-mail: epoc@cetuc.puc-rio.br

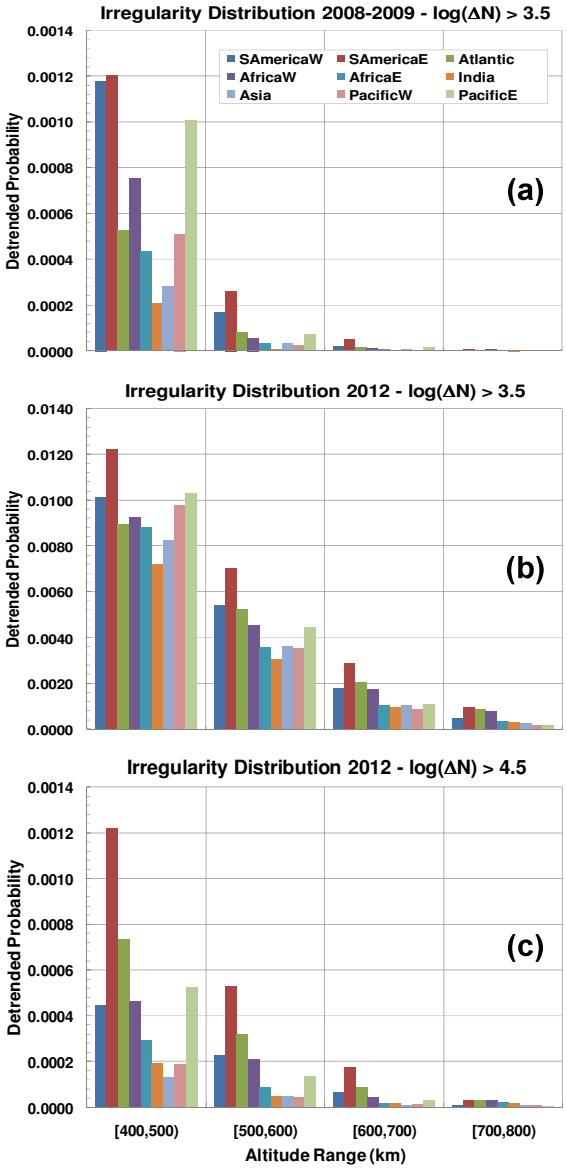

Figure 1. Probability distributions of ΔN_i as functions of altitude ranges and longitude sectors for: (a) 2008-2009 and $\log(\Delta N_i) > 3.5$; (b) 2012 and $\log(\Delta N_i) > 3.5$; (c) 2012 and $\log(\Delta N_i) > 4.5$.

Next, the combination of immediately available C/NOFS PLP data with a propagation model was used to forecast the scintillation index S_4 and the results compared with SCINDA VHF measurements at Ancon, Peru. Figure 2 plots the projections of the West and East links from the ground receiver to geostationary satellites, as well as their azimuths and elevations. Note that the

Emanoel Costa
Centro de Estudos em Telecomunicações/CETUC
Rua Marquês de São Vicente, 225 – Gávea
22451-900 Rio de Janeiro - RJ – Brasil
Tel: 55 21 3527 1682; Fax: 55 21 3527 1154
E-mail: epoc@cetuc.puc-rio.br

magnetic inclinations and declinations are very small and that Local Time is approximately equal to Universal Time minus 5 h in the Ancon region.

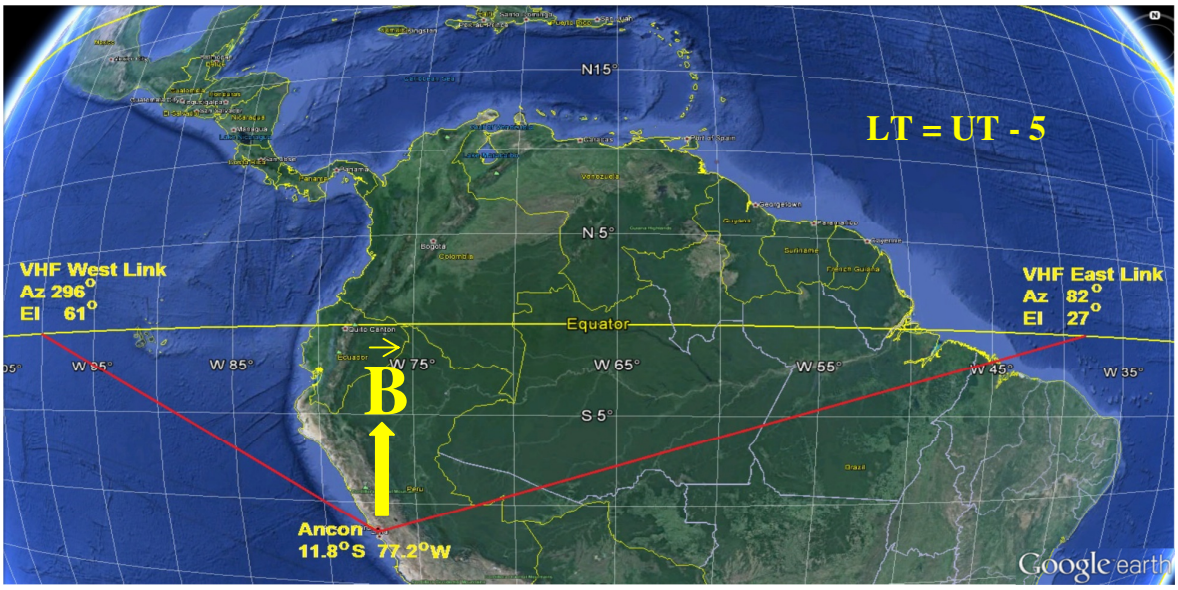

Figure 2. Projections of the West and East links from the ground receiver to geostationary satellites.

The left and right panels of Figure 3 plot the number of minutes with $S_4 > 0.4$ and $S_4 > 0.7$, respectively, for the West (blue) and East (red) links for each evening of the year 2009, during solar minimum conditions. The data availability is represented by the green curves and the right-hand side axes. Note that S_4 exceeded 0.4 during more than four hours an exceeded 0.7 during more than one hour for several evenings of the year 2009.

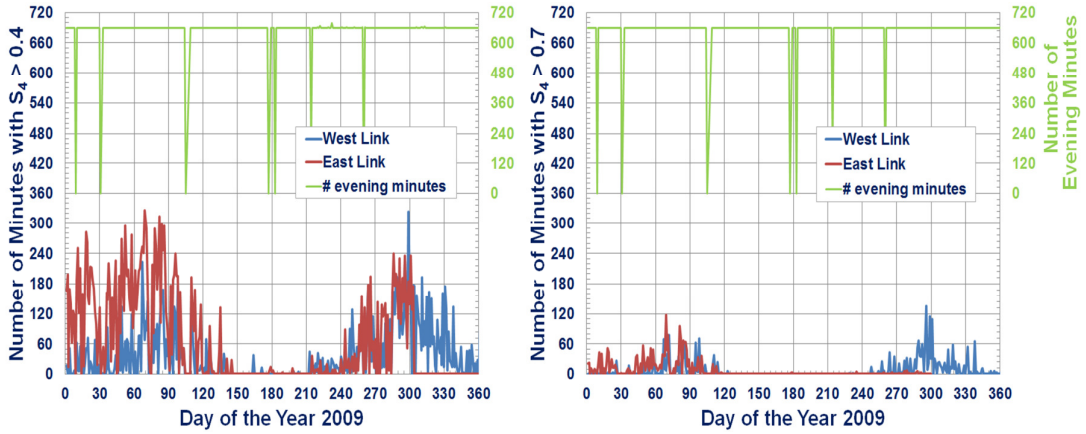

Figure 3. Number of minutes with $S_4 > 0.4$ (left) and $S_4 > 0.7$ (right) for the West (blue) and East (red) links for each evening of the year 2009. The data availability is represented by the green curves and the right-hand side axes.

Emanoel Costa
Centro de Estudos em Telecomunicações/CETUC
Rua Marquês de São Vicente, 225 – Gávea
22451-900 Rio de Janeiro - RJ – Brasil
Tel: 55 21 3527 1682; Fax: 55 21 3527 1154
E-mail: epoc@cetuc.puc-rio.br

Figure 4 displays the variation of S_4 with Universal Time during January 21 2012 and defines several scintillation events (red, a continuous period of time when S_4 exceeds a threshold) and interevents (green, a continuous period of time when S_4 remains below a threshold).

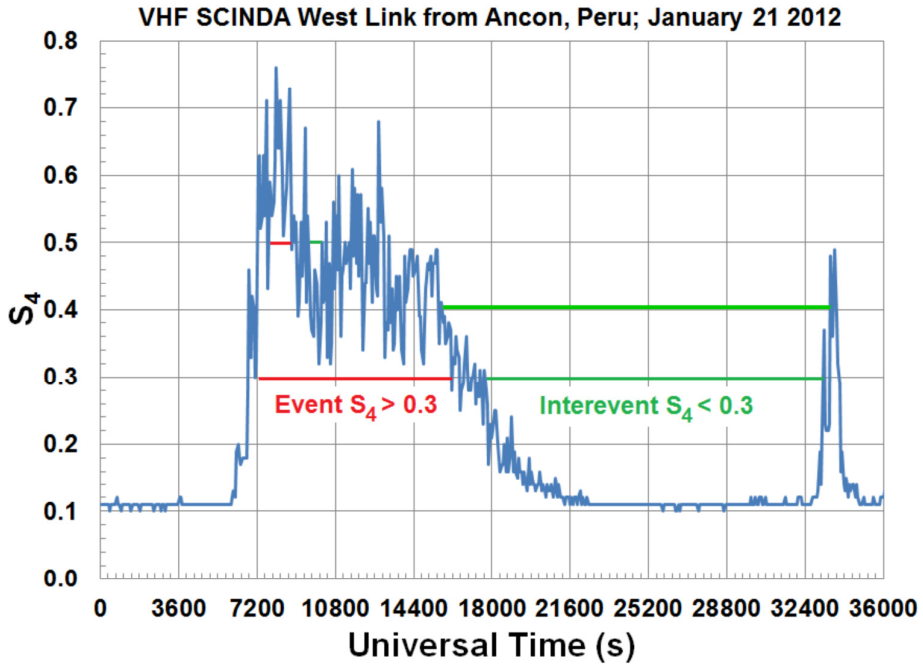

Figure 4. Variation of S_4 with Universal Time during January 21 2012 and definitions of scintillation events (red, a continuous period of time when S_4 exceeds a threshold) and interevents (green, a continuous period of time when S_4 remains below a threshold).

The upper left and right panels of Figure 5 plot the distributions of durations of events with $S_4 > 0.4$ and $S_4 > 0.7$, respectively. As expected, the number of events with $S_4 > 0.4$ is greater than the number of events with $S_4 > 0.7$, for the same duration. Similarly, the lower left and right panels of the same Figure display the distributions of durations of interevents with $S_4 < 0.4$ and $S_4 < 0.7$, respectively. Both Figures use results from the West link measurements during the year 2009. It is observed that most of the events and interevents are relatively short.

Emanoel Costa
Centro de Estudos em Telecomunicações/CETUC
Rua Marquês de São Vicente, 225 – Gávea
22451-900 Rio de Janeiro - RJ – Brasil
Tel: 55 21 3527 1682; Fax: 55 21 3527 1154
E-mail: epoc@cetuc.puc-rio.br

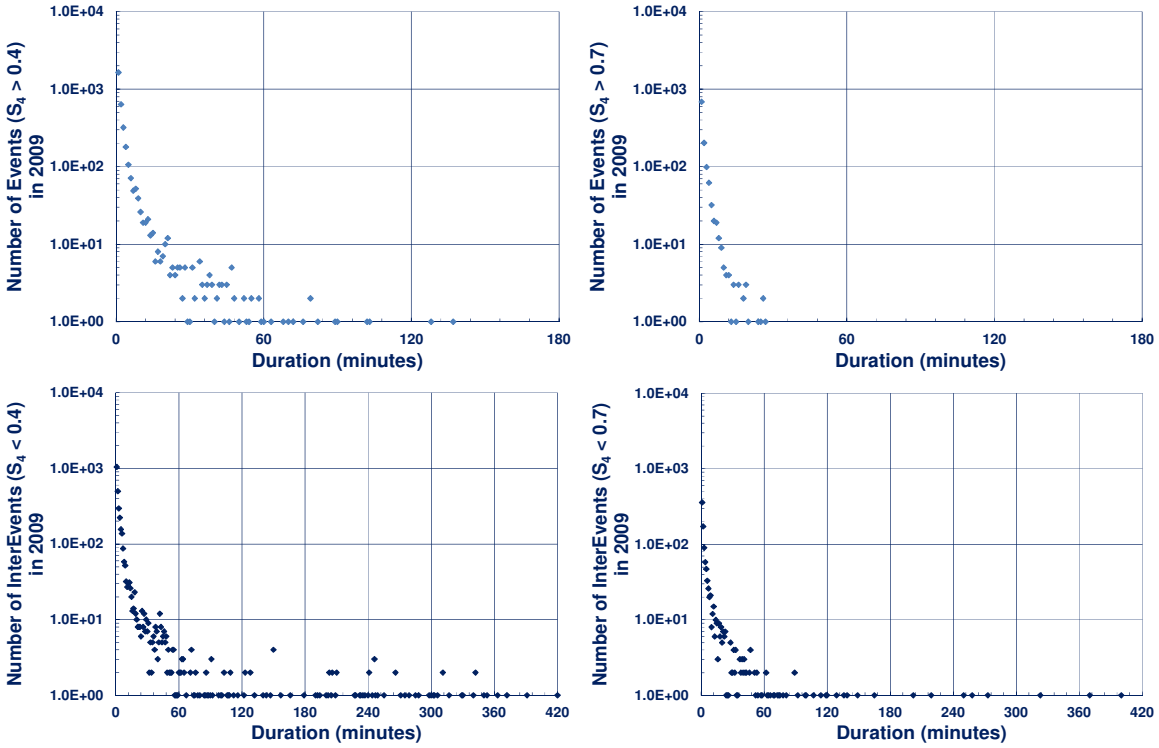

Figure 5. Distributions of durations of events with $S_4 > 0.4$ (upper left) and $S_4 > 0.7$ (upper right). Distributions of durations of interevents with $S_4 < 0.4$ (lower left) and $S_4 < 0.7$ (lower right).

Figure 6 sketches the scenario which supports the scintillation calculations performed by the model. It is assumed that field-aligned irregularities drift across the magnetic field with a drift velocity which is typically equal to V_{DRIFT} = 0.1 km/s. Thus, it can also be assumed that the C/NOFS satellite, orbiting with a velocity approximately equal to 7.5 km/s, detects a quasi-instantaneous pattern of irregularities over the receiver region. Considering the instant and position of detection of a sample of ΔN_i as well as V_{DRIFT}, the model determines the instant of time when the sample reaches the surface defined by the slant ray path and the intercepted magnetic field lines. Next, ΔN_i is scaled for altitude using the observed average ion density profile. That is, $\Delta N_i(400\ km) = [N_i(400\ km)/\ N_i(h)]\ \Delta N_i$. The scaled value $\Delta N_i(400\ km)$, fixed power spectral density parameters (outer scale wave number L_o = 12.5 km and spectral slope p = 1.7) and layer thickness L = 100 km are used to generate a horizontal random phase screen at the altitude of 400 km. Finally, the algorithm proposed by Costa and Basu [**Radio Sci.**, **37**(3), doi 10.1029/2001RS002498, 18.1-18.13, June, 2002] is used to numerically propagate a wave front to the ground and to estimate S_4. The above procedure is repeated for all the samples of the high-elevation sections of the C/NOFS satellite orbits over Ancon, Peru.

It should be observed that scintillation results from the contribution of irregularities which are distributed along the ray path. To account for the averaging effect of this distribution, S_4 time series derived from each orbit is smoothed by the application of a 30-minute running mean. The

Emanoel Costa
Centro de Estudos em Telecomunicações/CETUC
Rua Marquês de São Vicente, 225 – Gávea
22451-900 Rio de Janeiro - RJ – Brasil
Tel: 55 21 3527 1682; Fax: 55 21 3527 1154
E-mail: epoc@cetuc.puc-rio.br

results are then compared with the corresponding ones obtained from measurements performed by the SCINDA VHF West link at Ancon, Peru.

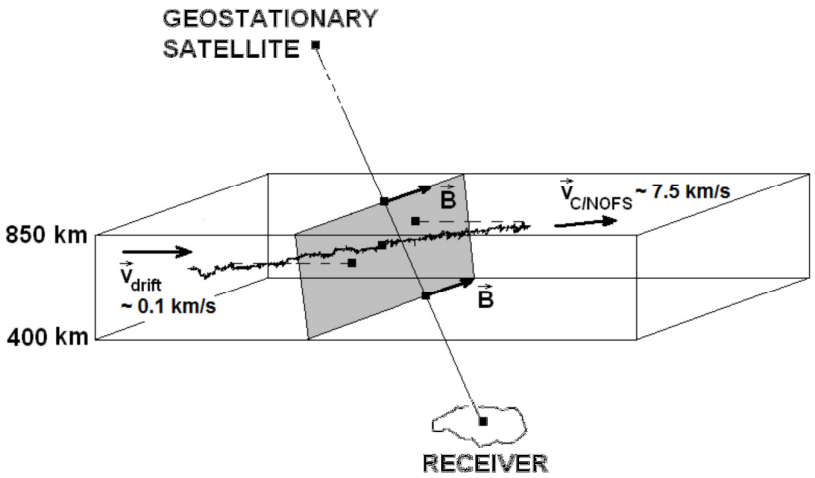

Figure 6. Scenario which supports the scintillation calculations performed by the model.

Figure 7 shows results from calculations (red) and measurements (blue) for two particular evenings of the year 2009. Note that three scintillation regimes were identified by the background color: weak (green, $S_4 < 0.4$); moderate (yellow, $0.4 < S_4 < 0.7$); and strong (red, $S_4 > 0.7$).

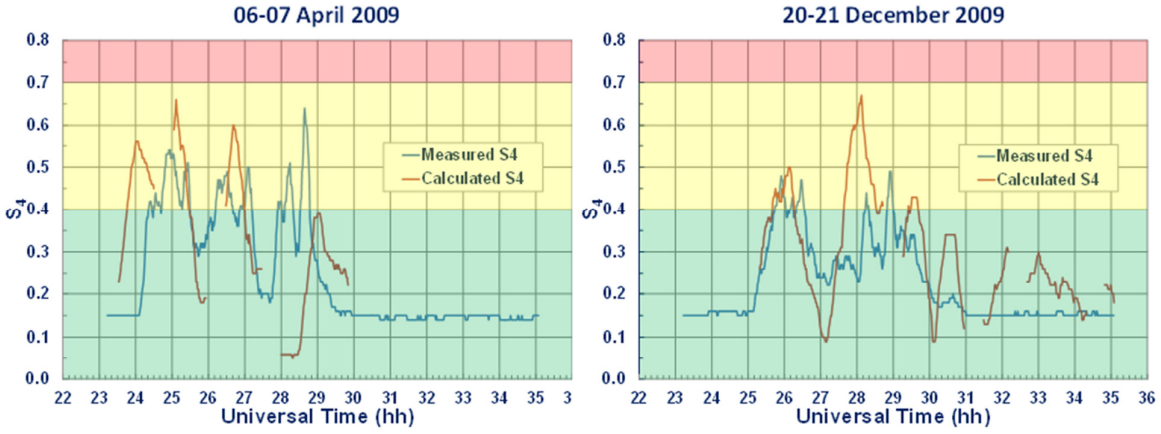

Figure 7. Comparison between results from calculations (red) and measurements (blue) for two particular evenings of the year 2009.

Emanoel Costa
Centro de Estudos em Telecomunicações/CETUC
Rua Marquês de São Vicente, 225 – Gávea
22451-900 Rio de Janeiro - RJ – Brasil
Tel: 55 21 3527 1682; Fax: 55 21 3527 1154
E-mail: epoc@cetuc.puc-rio.br

The distribution of errors (S_{4meas} - S_{4calc} at each instant of time) for the year of 2009 is displayed in Figure 8. The bin intervals are defined by (0.n – 0.05, 0.n + 0.05), where n is an integer between -7 and +9. Note that the error distribution is highly concentrated and slightly biased: the most probable value is 0.1.

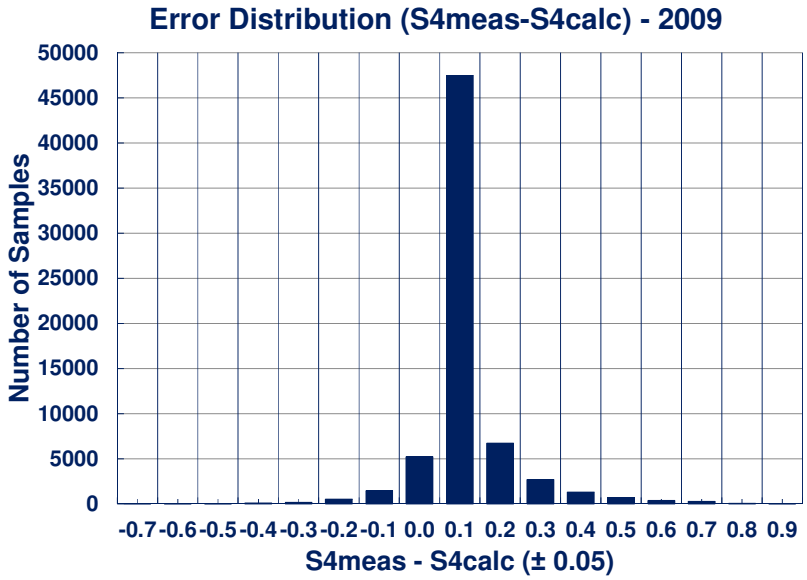

Figure 8. Distribution of errors (S_{4meas} - S_{4calc} at each instant of time) for the year 2009.

Table 2 distributes the calculated and measured values of S_4 into the three scintillation regimes (weak, moderate and strong) characterized above. The same results are represented by absolute values and percentages in the upper and lower parts of the Table 2, respectively. The agreement is better in the weak scintillation regime. The model underestimates or overestimates the severity of scintillation in 4.78 % (below the main diagonal) or 0.83 % (above the main diagonal) of the cases, respectively.

Table 2. Distribution of the calculated and measured values of S_4 into three scintillation regimes.

TOTAL: 67146	0.0 < S4calc < 0.4	0.4 < S4calc < 0.7	S4calc > 0.7
0.0 < S4meas < 0.4	63179	510	32
0.4 < S4meas < 0.7	2751	201	14
S4meas > 0.7	451	8	0

	0.0 < S4calc < 0.4	0.4 < S4calc < 0.7	S4calc > 0.7
0.0 < S4meas < 0.4	94.09 %	0.76 %	0.05 %
0.4 < S4meas < 0.7	4.10 %	0.30 %	0.02 %
S4meas > 0.7	0.67 %	0.01 %	0.00 %

Emanoel Costa
Centro de Estudos em Telecomunicações/CETUC
Rua Marquês de São Vicente, 225 – Gávea
22451-900 Rio de Janeiro - RJ – Brasil
Tel: 55 21 3527 1682; Fax: 55 21 3527 1154
E-mail: epoc@cetuc.puc-rio.br

Note that there are several uncertainty factors in the above calculations. For example, frozen-in and field-aligned irregularities were assumed. In situ measurements do not generally estimate the thickness of the irregularity layer and the values of the standard deviation were adjusted to consider the corresponding altitude. Additionally, fixed spectral representation of irregularities and drift velocity were assumed. In principle, spectral parameters and drift velocities could be estimated from instrumentation onboard the C/NOFS satellite. A better control of these uncertainty factors may improve the forecasting capability of the model.

Supported Personnel: Emanoel Paiva de Oliveira Costa (Principal Investigator, Associate Professor, CETUC PUC-Rio).

Publications: (1) Moraes, A. O., E. Costa, E. R. de Paula, W. J. Perrella, and J. F. G. Monico, Extended Ionospheric Amplitude Scintillation Model for GPS Receivers, **Radio Sci.**, **49**(5), 315-329, doi:10.1002/ 2013RS005307, May, 2014. (2) Costa, E, P. A. Roddy, and J. O. Ballenthin, Statistical Analysis of C/NOFS Planar Langmuir Probe Data, **Ann. Geophys.**, **32**, 773–791, doi:10.5194/angeo-32-773-2014, July 2014.

Interactions/Transitions: (1) 2013 Beacon Satellite Symposium (BSS 2013, Bath, UK, July 2013): presentation of two papers in Oral and Poster Sessions and review meetings on the project with Drs. Keith M. Groves (ISR/Boston College, Chestnut Hill, MA, USA) and Eurico R. de Paula (INPE, São José dos Campos, SP, Brazil); (2) 13th International Congress of the Brazilian Geophysical Society & EXPOGEf (13th CISBGf, Rio de Janeiro, RJ, Brazil, August 2013): co-chair of Session, presentation of paper in Oral Session and review meetings on the project with Drs. Keith M. Groves and Eurico R. de Paula; (3) Visit to the Air Force Research Laboratory (AFRL), Kirtland AFB, Albuquerque, MN, USA, December 2013: presentation of the Seminar "C/NOFS Planar Langmuir Probe Data: Statistical Analysis, Scintillation Predictions and Comparison with Ancon SCINDA Measurements" and review meetings on the project with AFRL researchers; (4) American Geophysical Union Fall Meeting 2013 (AGU Fall Meeting 2013, San Francisco, CA, USA, December 2013): presentation of invited talk in Oral Session; and (5) XXXI URSI General Assembly and Scientific Symposium (XXXI URSI GASS, Beijing, China, August 2014): presentation of the paper "Costa, E., P. A. Roddy, K. Wiens, and C. Valladares, Equatorial Scintillation Predictions from C/NOFS Planar Langmuir Probe Electron Density Fluctuation Data" in Oral Session and discussion of results with Drs. Sunanda Basu (Boston College) and Patricia H. Doherty (Boston College), as well as with researchers in the audience. Based on these interactions, the results will be reviewed and extended. The corresponding manuscript will be submitted for publication in Radio Science in the current calendar year.

New discoveries, Inventions, or Patent Disclosures: None

Honors/Awards: None

Emanoel Costa
Centro de Estudos em Telecomunicações/CETUC
Rua Marquês de São Vicente, 225 – Gávea
22451-900 Rio de Janeiro - RJ – Brasil
Tel: 55 21 3527 1682; Fax: 55 21 3527 1154
E-mail: epoc@cetuc.puc-rio.br